Available online at www.sciencedirect.com
ScienceDirect
Advances in Space Research xxx (2011) xxx–xxx
ADVANCES IN SPACE RESEARCH (a COSPAR publication)
www.elsevier.com/locate/asr

Imaging interplanetary CMEs at radio frequency from solar polar orbit

Wu Ji [a], Sun Weiying [a,*], Zheng Jianhua [a], Zhang Cheng [a], Liu Hao [a], Yan Jingye [a], Wang Chi [a], Wang Chuanbing [b], Wang Shui [b]

[a] Center for Space Science and Applied Research, Chinese Academy of Sciences, Beijing 100190, China
[b] School of Earth and Space Sciences, University of Science and Technology of China, Hefei 230026, China

Received 10 November 2009; received in revised form 25 April 2011; accepted 2 May 2011

Abstract

Coronal mass ejections (CMEs) represent a great concentration of mass and energy input into the lower corona. They have come to be recognized as the major driver of physical conditions change in the Sun–Earth system. Consequently, observations of CMEs are important for understanding and ultimately predicting space weather conditions. This paper discusses a proposed mission, the Solar Polar Orbit Radio Telescope (SPORT) mission, which will observe the propagation of interplanetary CMEs to distances of near 0.35 AU from the Sun. The orbit of SPORT is an elliptical solar polar orbit. The inclination angle between the orbit and ecliptic plane should be about 90°. The main payload on board SPORT will be an imaging radiometer working at the meter wavelength band (radio telescope), which can follow the propagation of interplanetary CMEs. The images that are obtained by the radio telescope embody the brightness temperature of the objectives. Due to the very large size required for the antenna aperture of the radio telescope, we adopt interferometric imaging technology to reduce it. Interferometric imaging technology is based on indirect spatial frequency domain measurements plus Fourier transformation. The SPORT spacecraft will also be equipped with a set of optical and in situ measurement instruments such as a EUV solar telescope, a solar wind ion instrument, an energetic particle detector, a magnetometer, a wave detector and a solar radio burst spectrometer.

Keywords: Interplanetary CMEs; Interferometric imaging; Solar polar orbit; Radio telescope

1. Introduction

Coronal mass ejections (CMEs) are expulsions of coronal plasmas and magnetic fields from the Sun. They occur at low heliographic latitudes. CMEs are responsible for the convection of magnetized solar plasmas into interplanetary space, with the fastest (>1000 km/s) CMEs typically causing the most intense interplanetary disturbances (Srivastava and Venkatakrishnan, 2002). Once very fast CMEs propagate toward Earth, geospace may be severely disturbed. The day side of the magnetosphere is compressed inward, even exposing geostationary satellites to the interplanetary solar wind without the protection of the magnetosphere. And Earth's magnetic field exhibits large variations over a short time period, called magnetic storms. These storms could cause ionospheric anomalies, interrupting satellite communications and introducing errors in satellite navigation signals. As CMEs propagate in other directions, they may interact with other planets (e.g., Mars), and may also cause problems for interplanetary spacecraft during deep space exploration. Therefore, the detection of CMEs is important for understanding and ultimately predicting space weather conditions (Bothmer and Daglis, 2007).

The Solar Polar Orbit Radio Telescope (SPORT) mission is proposed and studied by the Center for Space Science and Applied Research, Chinese Academy of Sciences, in 2004, and later jointly studied by the University of Science and Technology of China, National Astronomical Observatories and China Aerospace Science and Technology Corporation. It will image interplanetary CMEs and follow their propagation and evolution in the interplanetary space using interferometric imaging technology at the radio wave band from solar polar orbit. Measurements from SPORT will also

* Corresponding author.
E-mail address: sunweiying@nmrs.ac.cn (W. Sun).

0273-1177/$36.00
doi:10.1016/j.asr.2011.05.001

provide early warnings of CMEs, which are important for forecasting space weather events at the space stations, hundreds of application satellites and many other areas of human activities.

2. CME observations

Many efforts have been made since the 1960's to observe CMEs. The Seventh Orbiting Solar Observatory (OSO-7) was launched on September 29, 1971. The instruments carried on OSO-7 include White light coronagraph and Extreme Ultraviolet Corona Experiment. R. Tousey was the first to detect a CME on December 14, 1971, using OSO-7 (Howard et al., 2008). Skylab was launched on May 14, 1973. Skylab carried White light coronagraph on the Apollo Telescope Mount (ATM). Observations of CMEs have been obtained by the white light coronagraph and the first study of CME properties was performed (Gosling et al., 1974). Helios was launched on November 10, 1974 and January 15, 1976, respectively. The zodiacal light photometers on board the Helios spacecraft were used to form images of interplanetary CMEs from the vicinity of Earth's orbit to about 0.3 AU from the Sun (Jackson, 1985). The Space Test Program spacecraft (P78-1) or Solwind was launched on February 24, 1979. Solwind carried a Lyot white light coronagraph (Doschek, 1983). CMEs are observed by the Lyot white light coronagraph located outside the Earth's atmosphere. Solar Maximum Mission (SMM) was launched on February 14, 1980. The white-light coronagraph/polarimeter telescope (C/P) on aboard the SMM satellite observed to distances of 6 solar radii from Sun center, made first high-resolution observations of coronal mass ejections. Solar and Heliospheric Observatory (SOHO) was launched on December 2, 1995. SOHO carried a Large Angle and Spectrometric Coronograph (LASCO). LASCO observes corona from near the solar limb to a distance of 21 million kilometers (about one seventh of the distance between the Sun and the Earth). The Coriolis spacecraft was launched on January 6, 2003. The Solar Mass Ejection Imager (SMEI) on board it has been obtaining white light images of CMEs as they travel through the inner heliosphere (Tappin et al., 2004; Webb et al., 2006). In addition, observations of many thousands of CMEs have been collected from a series of space-borne coronagraphs (Michels et al., 1980; MacQueen et al., 1980; Brueckner et al., 1995). NASA's Solar Terrestrial Relations Observatory (STEREO) mission was launched on October 25, 2006. The Sun Earth Connection Coronal and Heliospheric investigation (SECCHI) on board STEREO consists of five telescopes. These telescopes are: an extreme ultraviolet imager, two traditional Lyot coronagraphs and two new designs of heliospheric imagers. With the launch of the Coriolis and the STEREO mission in 2003 and 2006, respectively, CMEs can now be observed remotely all the way to the Earth (Lugaz et al., 2010; Davis et al., 2009). Furthermore, without disturbance of ionosphere, another approach has used Interplanetary Scintillation (IPS) data to detect and track CMEs, both through analyzing their velocity as measured with multiple receiving stations, and through using the IPS level itself as a measure of the integrated density column (Asai et al., 1998).

3. Observing interplanetary CMEs from solar polar orbit

When CMEs are ejected from the Sun, initial speed plays an important role. However, once they enter interplanetary space, their structure takes the leading role in their subsequent evolution. During the following days, the structure of the plasma clouds changes greatly. The density of the clouds may not simply disperse; it may develop shocks, and the dense plasma clouds may pile up and leave density holes behind the piled front. However, these features are mostly predictions from modeling and simulations, with current direct in situ confirmation restricted to near 1 AU. Despite the attention paid by both the scientific community and government agencies to space weather issues in recent years, observation of interplanetary CMEs is the major weak point.

There are two flaws in the observation of interplanetary CMEs. The first is that the foregoing observations of CMEs are all obtained in ecliptic plane. If we observe interplanetary CMEs out of the ecliptic plane, the observations will be a helpful supplement for those observations that obtained in ecliptic plane. The second is that the foregoing observations of CMEs are recorded in EUV and white light band. And the programs than can observe the propagation of interplanetary CMEs are deficient. If we detect the emission brightness temperature of CMEs after they are ejected into interplanetary space with radio wave detectors, the observations will be a helpful supplement for those observations that are obtained in other wave bands. The scientific motivation of the SPORT mission is to reveal how interplanetary CMEs propagate by use of the radio wave detectors from solar polar orbit.

SPORT will be the first mission to image the propagation and evolution of ICMEs continuously from out of the ecliptic plane. It will accelerate the development of reliable space weather forecast techniques. The principal mission objective for SPORT is to trace the propagation and evolution of CMEs. Specific science objectives are to:

- Characterize the propagation and evolution of CMEs and possibly understand the characteristics of CIR.
- Establish the physical model and prediction model of interplanetary space and geospace weather in response to CMEs and their interplanetary disturbance responses.
- Detect solar short-time radio bursts and develop the physical model of interplanetary space weather in response to these bursts.
- Develop a time-dependent model of the magnetic topology, temperature, density, and velocity structure of the ambient solar wind.
- Understand the interaction process of magnetic field and plasmas.

Please cite this article in press as: Wu, J., et al. Imaging interplanetary CMEs at radio frequency from solar polar orbit. J. Adv. Space Res. (2011), doi:10.1016/j.asr.2011.05.001

The SPORT mission will provide a completely new perspective of CMEs by remote sensing in a radio wave band from solar polar orbit. It will track CMEs to distance of near 0.35 AU from the Sun. SPORT's high latitude position will ease the study of west-east deflection propagation. When viewed from SPORT, Earth-directed CMEs will appear as limb CMEs, this can be used to predict if & when CMEs arrive at Earth. Furthermore, the question of whether Earth, Mars or any deep space missions might be affected by CMEs could be answered more clearly.

4. The SPORT mission

The two main themes of the SPORT mission are the use of the radio wave band and the observation from the solar polar orbit. The main radio telescope on board the SPORT mission will image CMEs as they propagate in interplanetary space. The radio telescope is an interferometric synthetic aperture radiometer. In aperture synthesis, one utilizes several small antennas in combination with signal processing techniques in order to obtain resolution that otherwise would require the use of an antenna with a large aperture. In this technology the coherent correlations of signals from pairs of antennas are obtained at different antenna-pair spacings (baselines). The correlation for each baseline yields a sample point in a Fourier transform of the brightness temperature map of the objective. An image of the objective itself is then reconstructed by inverting the sampled transform. Only this resulting image need be transmitted back to Earth, thus significantly reducing telemetry requirements for SPORT's distant-from-Earth orbit.

Before proceeding with the engineering design, the first question to answer is which frequency band should be chosen to obtain images of CMEs. Because we aim to track the propagation of CMEs continuously, short radio bursts produced by CMEs are not reliable foundations for selecting the observation frequency. Analysis of the plasma clouds emitted by CMEs confirms that thermal free–free emission and gyrosynchrotron emission are the two major non-transient emissions that we should consider in designing the radio telescope.

Selection of the observation frequency for the main radio telescope involves a trade-off between the possible tracking distance from the Sun and the engineering feasibility of the antenna aperture of the telescope on the spacecraft. Due to the very large size required for the antenna aperture, the only practical technology is interferometric imaging technology, which is widely used on the ground for radio astronomy and has also been used in airborne and space-borne Earth observation in recent years. Interferometric imaging technology is based on indirect spatial frequency domain measurements plus Fourier transformation. Since the spatial frequency domain samples can be taken by a number of two-element interferometers with different baselines and one antenna element can be chosen many times to form different baselines, the telescope antenna array can be thinned substantially. To further reduce the complexity of the telescope antenna system, a time-shared rotation scan scheme that is called a clock-scanning system is introduced. The system starts with two-element antennas mounted on the far ends of two long booms extended from the spacecraft. The lengths of the two booms are slightly different, and the booms rotate at different speeds, like the minute and second hands of a clock. Because the two booms rotate at different angular speeds, the distance and orientation of the baselines formed by the two-element antennas mounted on the far ends of the booms vary, covering all sampling points in the spatial frequency domain (called the u–v plane). This basic two-element clock-scan configuration can be extended to more complicated schemes, like a 2–2 system with two 'minute' and two 'second' arms or a 4–4 system with four 'minute' and four 'second' arms. We propose to adopt the latter configuration for the main radio telescope of SPORT. An image retrieval algorithm is also being developed to adopt the new scan scheme.

Orbit injection to solar polar orbit is also difficult. The Ulysses mission demonstrated the possibility by using of the Jupiter gravity assist technology to escape from the ecliptic plane to the solar polar orbit. The ideal orbit for SPORT would not be as far from the Sun as Jupiter, which would give an aphelion of up to 5 AU. However, no other existing technology can provide a closer orbit with a relatively brief cruise period to reach the observation position.

The general requirements for the SPORT mission are the following:

1. The orbit of SPORT should be a solar polar orbit. In order to have an overall view to observe interplanetary CMEs, the inclination angle should be near 90°. In order to stay in the observation region as long as possible and at the same time to retain a reasonable spatial resolution, the aphelion of the orbit should be around 1–1.5 AU above the North Pole, and the perihelion should be around 0.5 AU. To set the aphelion over the North Pole is because that most of the ground receiving stations are located on the northern hemisphere of the Earth.
2. The main telescope of SPORT should have a minimum spatial resolution better than 0.05 AU in the ecliptic plane, and its field of view must cover most of the inner interplanetary space, i.e., within 0.5 AU.
3. The image refresh time should be no longer than one hour. CMEs generally propagate from the Sun to the Earth in about 2.5–3.5 days. An image refresh time of one hour would give 30–42 frames over the 0.5 AU inner interplanetary space. A refresh time of 1/2 h would be better, if technologically feasible.
4. Images should be sent back to the ground in real-time or quasi-real-time for the purpose of space weather forecasting. With this ability, we can provide geospace event forecasts from one to two days in advance.

Please cite this article in press as: Wu, J., et al. Imaging interplanetary CMEs at radio frequency from solar polar orbit. J. Adv. Space Res. (2011), doi:10.1016/j.asr.2011.05.001

The above requirements give the mission designers a basic picture of the SPORT mission. This four-point general design template will be carried throughout the assessment and key technology studies.

5. Frequency selection of the main radio telescope

The main radio telescope is the key scientific payload of the SPORT mission. It should be able to image interplanetary CMEs from right after they leave the surface of the Sun out to a distance of about 0.35 AU. The main telescope will detect the radio emission brightness temperature of interplanetary CMEs. Since the density of plasmas of interplanetary CMEs disperses during propagation in general, the thermal radio emission brightness temperature will decrease gradually as the CMEs depart from the Sun. And the higher the emission frequency is, the lower the emission brightness temperature will be (Sun and Wu, 2005). This implies that in order to track CMEs from solar corona to as far as possible, the observation frequency must be very low.

It is also obvious that lower frequencies require a large antenna if the spatial resolution requirement is kept the same. Therefore, the frequency selection involves a trade-off between the how far we can detect the radio emission of CMEs from the Sun and the technical feasibility of deploying a large antenna aperture in space.

Interplanetary CMEs may exhibit three relevant radio emission mechanisms: thermal free–free emission, gyrosynchrotron emission and plasma emission (Vourlidas, 2006). Among these emission types, thermal free–free emission is the main emission mechanism of the high-density plasma clouds of interplanetary CMEs. Gyrosynchrotron emission is the continuous emission generated by high-energy electrons from CMEs, while plasma emission is the main mechanism of transient radio bursts from CMEs. Since the main SPORT telescope is meant to continuously trace the propagation of interplanetary CMEs as far as possible, only the non-transient radio emissions, i.e., thermal free–free emission and gyrosynchrotron emission, are of interest.

5.1. Free–free emission

Free–free emission is produced by Coulomb collisions between charged particles in plasmas. It is one of the main radio emission mechanisms of thermal electrons of interplanetary CMEs.

The electron density model of background solar wind is given by the following equation (Leblanc et al., 1998):

$$n_e(R) = (7.2R^{-2} + 1.95 \times 10^{-3}R^{-4} + 8.1 \times 10^{-7}R^{-6})\ (\mathrm{cm}^{-3}). \quad (1)$$

With R in units of AU.

The electron temperature of background solar wind is given by Eq. (2) (Sittler and Scudder, 1980):

$$T_e = 5.5 \times 10^4 \times n_e^{0.175}\ (\mathrm{K}). \quad (2)$$

From the data that were obtained by SMM (St Cyr and Burkepile, 1990), the electron density of CMEs at 1 AU is probably 2–5 times larger than that of background solar wind.

Moreover, the electron density is inversely proportion to the propagating distance. Therefore, we evaluate the electron density of CMEs by the following equation:

$$n_{CME}(R) \approx (2\text{–}5) \cdot R^{-1} \cdot n_e(R). \quad (3)$$

With the data of SOHO/UVCS, Gopalswamy and Kundu estimated the plasma electron temperature of interplanetary CMEs as follows (Markus, 2004):

$$T_{CME} \approx (10^{4.5}\text{–}10^{5.5})\ \mathrm{K}. \quad (4)$$

The interplanetary magnetic field model from corona to 1 AU is given by the following equation (Tu, 1988):

$$B = B_0\left(\frac{1}{R}\right)^2\left[1 + \left(\frac{2\pi R R_\Theta}{TV}\right)^2\right]^{1/2}, \quad (5)$$

where $B_0 = 2$ G, $T \approx 2.2 \times 10^6$ s, V is the solar wind velocity, R_Θ is the radius of the Sun.

The magnetic field of interplanetary CMEs is much higher than those of cosmic background (Kivelson and Russell, 1995; Lepping et al., 1990). In this paper, it is estimated by the following equation:

$$B_{ICME} = 10B = 10B_0\left(\frac{1}{R}\right)^2\left[1 + \left(\frac{2\pi R R_\Theta}{TV}\right)^2\right]^{1/2}. \quad (6)$$

According to Eqs. (1)–(4), the brightness temperatures of thermal free–free emission of background solar wind (a) and of interplanetary CMEs are shown in Fig. 1.

Fig. 1(a) shows that, during the quiet Sun period (i.e., when only the background solar wind is present), the emissions even at low-frequency bands are obscured. Fig. 1(b) shows that, during CMEs propagating period, the emissions of CMEs are strong enough to be detected to distances of near 0.35 AU from the Sun at frequency no more than 150 MHz with an instrument which sensitivity is less than 1 K. From these calculations, a range from 15 to 150 MHz is therefore selected as the observation frequency for the main telescope of SPORT.

5.2. Gyrosynchrotron emission

Gyrosynchrotron emission is the electromagnetic emission generated by mildly relativistic electrons moving in a magnetic field (Ramaty, 1969). It is one of the main radio emission mechanisms of high-energy electrons from interplanetary CMEs.

Gradual solar energetic particle events associate closely with coronal mass ejections (Lario, 2005; Gopalswamy et al., 2002; Kahler et al., 2001). Protons and electrons are the primary composition of the solar energetic particles. The energy spectral index of the electrons is usually from

Please cite this article in press as: Wu, J., et al. Imaging interplanetary CMEs at radio frequency from solar polar orbit. J. Adv. Space Res. (2011), doi:10.1016/j.asr.2011.05.001

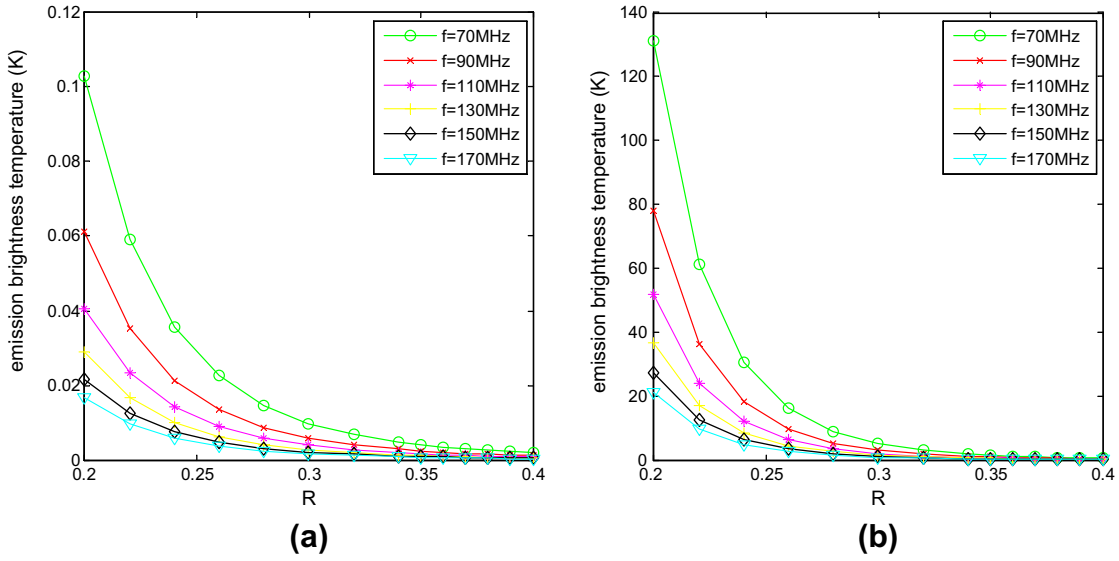

Fig. 1. Thermal free–free emission of background solar wind (a) and of interplanetary CMEs (b). R is the heliocentric distance; f is the emission frequency.

1.3 to 7 (Yao and Yu, 1998; Mewaldt, 2006; Markus, 2004; Wu et al., 2004). The electron density of the solar energetic particles that are moving together with CMEs is far less than that of CME's. In this paper, it is estimated by the following simple expression:

$$n_{high\text{-}energy\text{-}particles} \approx 10^{-2} \cdot n_{CME}(R). \quad (7)$$

The calculated results of the non-thermal gyrosynchrotron radiation of the solar energetic particles at $R = 0.5$ AU are given in Fig. 2. The view angle θ is the angle that between the observation direction and the magnetic field direction. In this calculation, we choose $\theta = \pi/3$.

It is shown in Fig. 2 that the non-thermal gyrosynchrotron radiation from the high-energy electrons is affected by the emission frequency, energy spectral index and view angle. The polarization characteristic of the emission is levorotatory circular polarization. The emission brightness temperature is strong enough to be detected from solar corona to near 0.5 AU as the emission frequency is more than 10^6 Hz.

Cosmic-background emission, galactic-background emission and solar radio emission should also be taken into account as we select the observation frequency of the SPORT mission. The measured value of the cosmic-background emission from 15 to 300 MHz is about 3 K (Sironi and Celora, 1990). The measured value of the galactic-background emission from 15 to 300 MHz is about from 10^4 to 50 K, which decreases sharply as frequency increasing, as shown in Fig. 3 (Manning and Dulk, 2001; Lemarchand, 1998). The measured value of the solar emission from 15 to 300 MHz is about 10^6 K. The Sun is a point source. Considering all these factors, we can determine that an observation frequency of 150 MHz will provide images of CMEs at a distance of 0.35 AU. And the propagating path of CMEs from greater than 0.35 to near 1 AU can be estimated by using of those data that are to be obtained by SPORT.

6. Design of the main telescope

From the above calculations, the working frequency can be selected in the VHF band at 150 MHz. Together with the observation frequency, the other fundamental requirements are given in Table 1.

The observation frequency bandwidth should be as wide as possible without introducing too many technical difficulties to the system. The polarization mode is selected to be circular polarization. The field of view (FOV) is determined from the pattern of the element antennas in the system. Due to the very long wavelength (2 m at 150 MHz), helical antennas are chosen to get an overall view of inner interplanetary space from a distance of a few solar radii to near 0.5 AU. The FOV is about ±25°.

The spatial resolution in the ecliptic plane is determined by the general size of CMEs. When they are close to the Sun, higher resolution is required. When they are near 0.35 AU, a much coarser resolution is adequate. A balanced requirement is 0.1 AU. If the observation distance is about 1.5 AU above the pole of the Sun, an angular spatial resolution of about 2° is required. A 60-m real antenna aperture can give an angular spatial resolution of about 2°. Using interferometric imaging technology, a 30-m physical aperture is equivalent to a 60-m real aperture. And using current technology, a physical antenna aperture of 30–40 m can be realized.

The image refresh cycle is a specification related to spatial resolution. These factors are related to the propagation velocity of CMEs in interplanetary space. Since slow CMEs travel from the Sun to the Earth in 36–48 h, they take 3.6–4.8 h to move a distance of 0.1 AU. While fast CMEs can travel from the Sun to the Earth within 24 h,

Please cite this article in press as: Wu, J., et al. Imaging interplanetary CMEs at radio frequency from solar polar orbit. J. Adv. Space Res. (2011), doi:10.1016/j.asr.2011.05.001

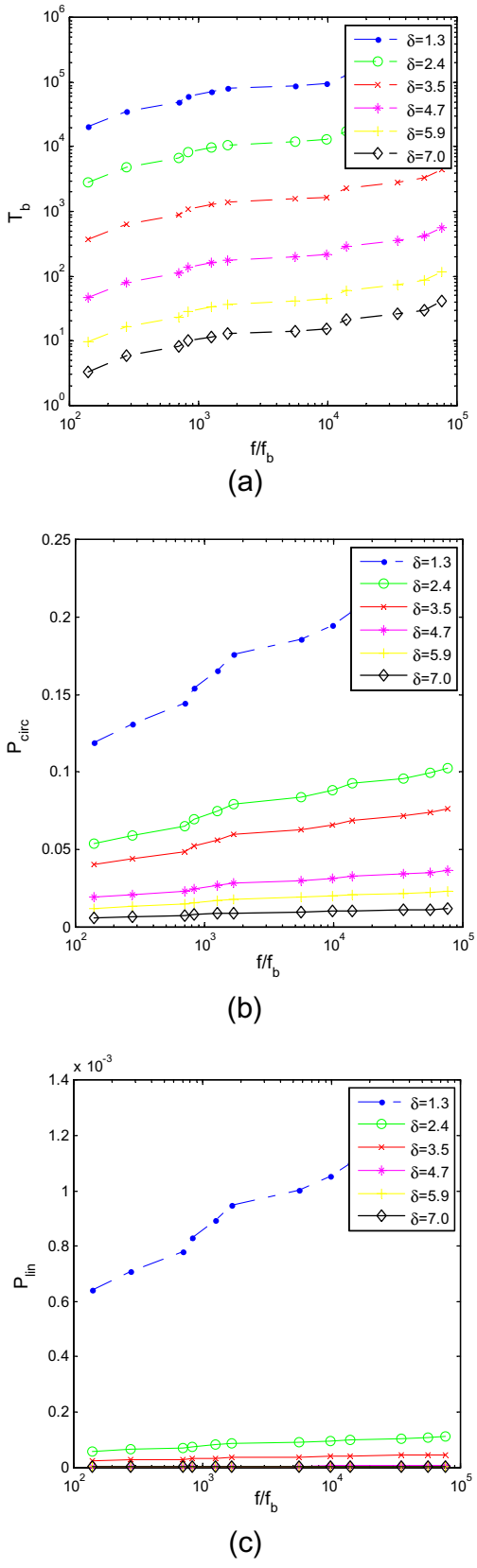

Fig. 2. Non-thermal gyrosynchrotron emission brightness temperature T_b (a), the degree of circular polarization P_{circ} (b) and the degree of linear polarization P_{lin} (c). f is the emission frequency; f_b is the cyclotron-frequency and equal to 7.188×10^3 Hz; δ is the energy spectral index of the electrons.

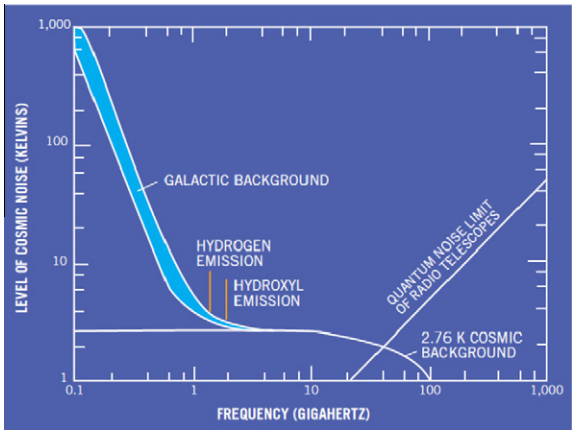

Fig. 3. Cosmic radio spectrum (Manning and Dulk, 2001; Lemarchand, 1998).

Table 1
Fundamental requirements to the main telescope.

Observation frequency and bandwidth	150±10 MHz
Polarization mode	Circular
FOV	±25°
Spatial resolution in the ecliptic plane	~2°
Imaging refresh cycle	⩽30 min
Sensitivity	<1 K

they take 2.4 h to move a distance of 0.1 AU. In order to produce a moving picture of CMEs while they travel through interplanetary space, the image refresh cycle should be ten times faster than the rate of change within one resolution pixel, i.e., 15–30 min.

The final fundamental specification is a key factor for a radiometer that determines the ability of the instrument to distinguish the targets from the background noise. Once the image refresh cycle is determined, the remaining ways to increase sensitivity are to use better receivers and to broaden the receiving channel bandwidth. The minimum requirement is to reach 1 K sensitivity; however, we will try to obtain the highest resolution that can be realized using current technology.

6.1. Basic theorem of interferometric imaging technology

Interferometric imaging technology was developed in the 1950s–1960s (Thompson et al., 1986) to increase the spatial resolution of telescopes in the radio and microwave frequency bands. The basic principle is to measure indirectly: not in the spatial domain but in the spatial frequency domain, called the u–v plane. After measurement, a Fourier transform is performed to obtain an image of the original scene. The quantity that is measured in the Fourier domain is called the Visibility Function. This name was retained when the technology was introduced to the area of Earth observation in the 1980s (Ruf et al., 1988).

Please cite this article in press as: Wu, J., et al. Imaging interplanetary CMEs at radio frequency from solar polar orbit. J. Adv. Space Res. (2011), doi:10.1016/j.asr.2011.05.001

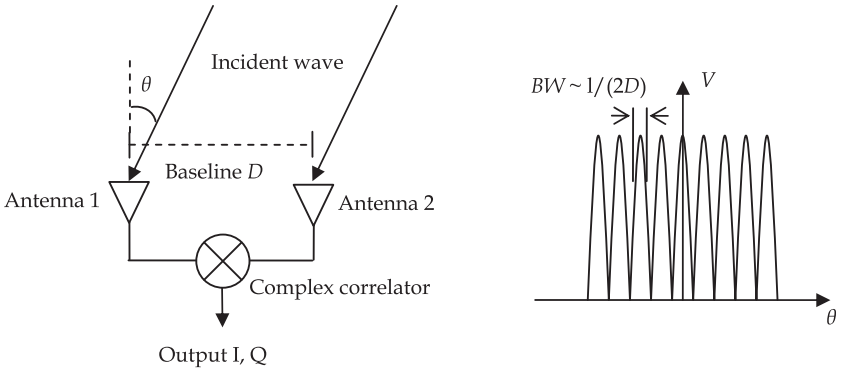

(a) Block diagram of an interferometer (b) Pattern of an interferometer

Fig. 4. Schematic diagram of two-element interferometer (a) and its pattern (b). BW is the bandwidth.

The measurements, called samplings, in the spatial frequency domain can be carried out using two coherent receiving channels with small element antennas and a complex correlator, as shown in Fig. 4.

'Coherent receiving channels' means that they use the same local oscillator. The complex correlator carries a multiplication function of the output signals from the two receivers and gives two outputs, I and Q, that represent the real part and the imaginary part of the complex value of the multiplication output. The two small element antennas form a baseline in space. The length of the baseline (the distance between the phase centers of the two antennas) represents the radius of a sampling point in the u–v plane, while the orientation of the baseline represents the polar angle of this sampling point in the u–v plane. A sampling point is exclusively defined by these two values, the module and the polar angle. In practice, each element can be used more than once to take many samples while combining with other elements to form different baselines. In this way, the antenna array composed of small elements can be much thinned. A Y-shaped two-dimensional liner array can represent a full 2-D array. There is no need to scan the antennas mechanically, since the field of view of this system is determined by the element antenna pattern, which already covers a wide area.

Another attractive nature of interferometric imaging technology is that the physical aperture of the thinned array can be reduced by half compared with traditional radiometers. This is because the beam width of each grating lobe of the interferometer is only half that of a traditional two-element array in which the outputs of the two elements are added, not multiplied. A mathematical explanation will be given in the following section.

We cannot use the Y-shaped array configuration because the physical aperture of the antenna array is too large. Such a large structure could not be folded during launch and deployed after the spacecraft is in orbit. Therefore, the number of elements must be reduced further.

Recently, a time-shared scanning scheme with low hardware complexity has attracted attention. This scheme has the potential to overcome the problems caused by bulky and complex hardware. In such a scheme, a few antenna elements are applied to compose a simple array, and the array may be moved integrally or the elements may be moved separately to obtain more spatial frequency samples. After each scanning cycle period, full u–v sampling coverage

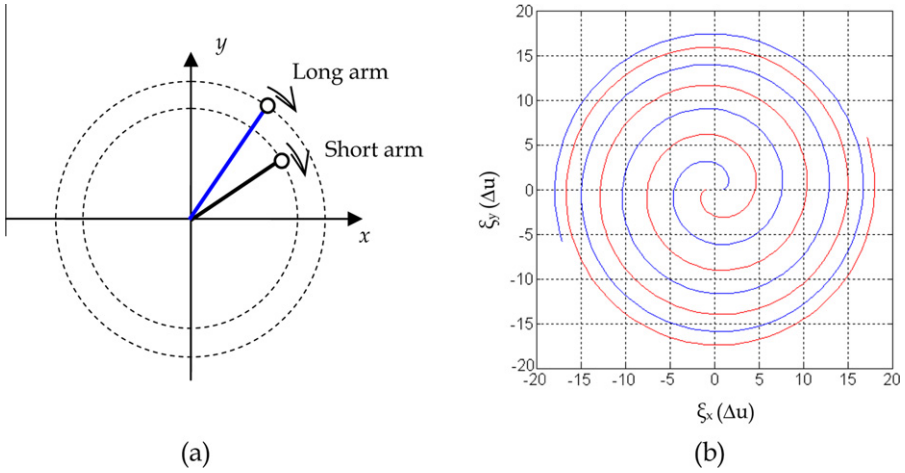

(a) (b)

Fig. 5. Schematic diagrams of clock scan scheme with two elements (a) and its sampling scanning trajectory in u–v plane (b).

Please cite this article in press as: Wu, J., et al. Imaging interplanetary CMEs at radio frequency from solar polar orbit. J. Adv. Space Res. (2011), doi:10.1016/j.asr.2011.05.001

can be achieved, and the brightness temperature image can be reconstructed by inversing the saved u–v measurement data. The time-shared scanning scheme can greatly reduce the number of antenna elements and receivers.

A new scanning scheme called clock scanning is even more suited for our requirements. The antenna elements are divided into two groups. The two groups rotate separately around the same axis with different angular rotation speeds. The elements in each group have the same angular rotation speed and arm length, but differ from the elements in the other group. This configuration is similar to a clock, especially when each group has only one antenna element, so it is called a clock scan (Wu et al., 2007); see Fig. 5(a).

The scanning tracks of the sampling points on the u–v plane of the clock scan scheme are spiral curves, as shown in Fig. 5(b). The uniformity and average gaps between the spirals are primarily determined by the speed ratio between the two antenna groups. As the speed ratio approaches 1, the sampling grid becomes more uniform and the scanning cycle period becomes longer. The largest and shortest baselines of clock scan scheme are, respectively determined by the sum and difference of the lengths of the long and short arms. Any length of baseline between the shortest and largest baselines can be created by the two antenna groups during their rotating scan. Therefore, the system complexity can be reduced to the simplifying limit of only two antenna elements and receivers. With this configuration, the clock scan can still conveniently and efficiently achieve full u–v sampling coverage. This is the most outstanding advantage of the clock scan. However, the scanning cycle period will be very long.

6.2. Preliminary design of the main telescope

Using the clock scan scheme, the main telescope will have two groups of element antennas and their receiving channels, each composed of four elements. A basic configuration is shown in Fig. 6.

The output of each helical antenna is connected to an independent receiver as shown in Fig. 7. The noise signals will be amplified directly up to the level suitable for digitization without any down converting. Clocks for digital A/D converter for all receiving channels are synchronized from a central clock located in the spacecraft and broadcast to all receivers by wireness communication.

The telescope aperture is composed of eight long booms. Group 1 consists of four 16-m booms that rotate together with the spacecraft. The rotation axis points towards the Sun, so the spacecraft is spin-stabilized. Group 2 also consists of four booms; these are 14 m long and rotate seven times slower than the spacecraft. However, using the spacecraft coordinates, Group 2 is the only rotating part of the telescope, with a rotation speed of two rotations per hour. This gives an image refresh cycle of 30 min. Since the spacecraft rotates seven times faster than Group 2, the spin speed of the spacecraft together with Group 1 is fourteen rotations per hour, roughly 4 min per rotation.

As shown in Fig. 7, the digitized noise signals are transmitted to the spacecraft by the cable. On the spacecraft, the communication system passes the noise signals from eight receivers to the main processor, where the interferometric samples are calculated. Once the samples are obtained, an image retrieval algorithm is performed to produce the

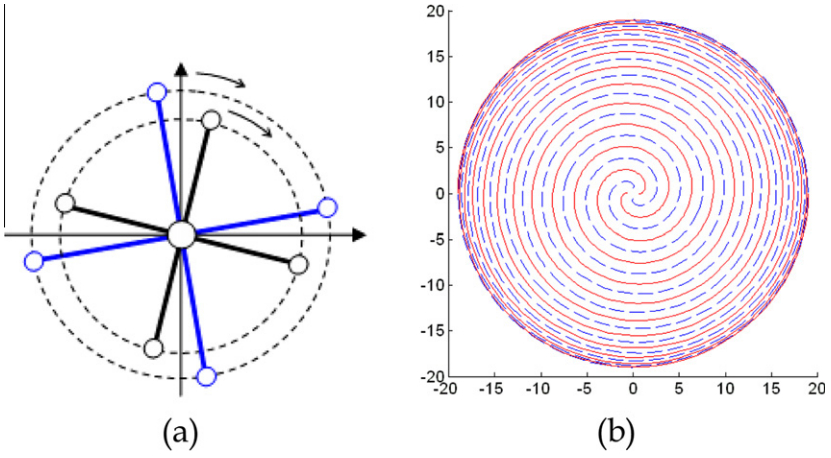

Fig. 6. 4 + 4 arms clock scan system (a) and its sampling tracks on the u–v plane (b).

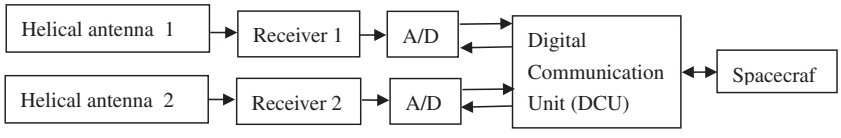

Fig. 7. Element receiving channels of the main telescope.

Please cite this article in press as: Wu, J., et al. Imaging interplanetary CMEs at radio frequency from solar polar orbit. J. Adv. Space Res. (2011), doi:10.1016/j.asr.2011.05.001

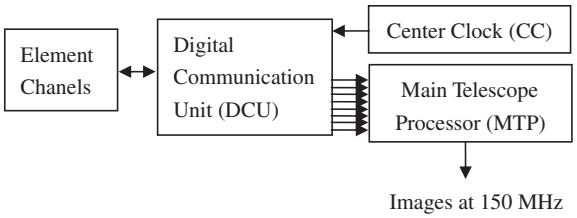

Fig. 8. The transfer process of the noised signals from element channels to the main telescope processor.

image. Only the retrieved image is sent to the ground station on Earth. Therefore, the telemetry requirement is not high and will not be a key problem for spacecraft engineering design. The transfer process of the noised signals from element channels to the main telescope processor is shown in Fig. 8.

6.3. Image retrieval algorithm

The MTP performs cross correlations and retrieves the image. The image retrieval algorithm can be divided into two parts including an interpolation and a fast Fourier transformation (FFT).

For the clock scan scheme, the sampling points are not located in a rectangular grid. They are located in a spiral grid, which is nearly a polar grid. In contrast to rectangular grids, for polar grids and spiral grids sampled by a rotation scanning system, no fast direct algorithm exists for Fourier transformation. However, an interpolation method can be applied to convert these irregular girds into a uniform grid for reconstruction via FFT routines. This is called the interpolation-based Fourier method. Two major interpolation based Fourier methods have been proposed: the rectangular grid based Gridding method (Beatty et al., 2005) and the pseudo-polar grid-based 1-D interpolation pseudo-polar FFT method (Zhang et al., 2007).

The Gridding method is a convolution-based re-sampling technique that is widely used to convert random non-uniform data into a rectangular grid. The procedure first estimates the sampling density of the non-uniform data and compensates the data by dividing their density; then the compensated data are convolved with a specific kernel function to recover the corresponding initial function and resample it on the required Cartesian grid. Finally, a standard IFFT is performed to reconstruct the brightness temperature image. The density estimation and convolution kernel are the most important factors for reconstruction accuracy. Generally, the Voronoi diagram method can be used to calculate the sampling density, and the widely accepted Kaiser–Bessel kernel function can be used to do the convolution.

The interpolation pseudo-polar FFT method is specifically proposed for the polar grid of concentric circles sampled by a synchronous rotation scanning system. The 1-D interpolation pseudo-polar FFT method uses two steps of 1-D interpolations: angular interpolation and radial interpolation. The polar grid can be converted to a pseudo-polar grid that is composed of concentric rectangles and equi-sloped rays. Then, by applying 1-D FFT and fast FRFT (fractional Fourier transform), the spatial frequency data in the pseudo-polar grid can be transformed to a Cartesian grid in the spatial domain.

The interpolation pseudo-polar FFT method gives promising imaging performance by virtue of the high accuracy of 1-D interpolation and fast computational operation. Fig. 9 shows the interpolating process and the pseudo-polar grids.

7. Orbit design of SPORT

The current technical level can not realize the ideal orbit that is mentioned in Section 4. However, an existing solar polar orbit has been used by Ulysses. The orbit of SPORT is designed to follow the Ulysses orbit with the Jupiter gravity assist to get enough energy to escape from the ecliptic plane. Fig. 10 shows the SPORT orbit.

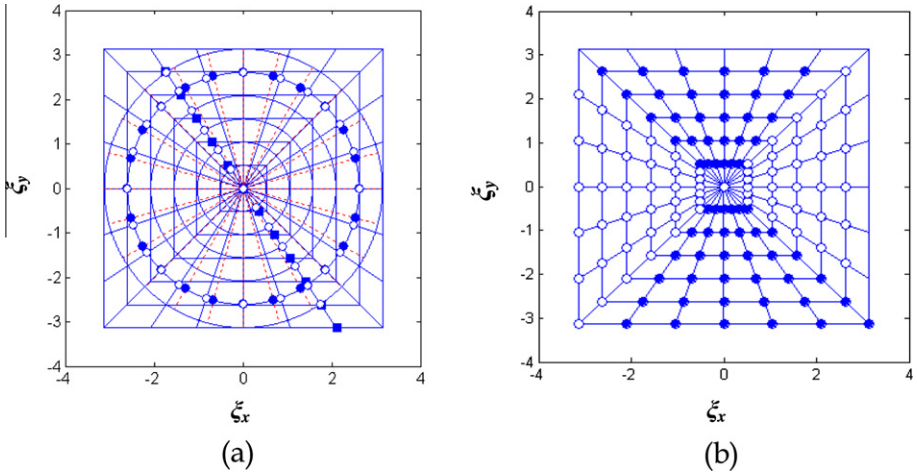

Fig. 9. Pseudo-polar interpolating process (a) and the final grid points (b).

Please cite this article in press as: Wu, J., et al. Imaging interplanetary CMEs at radio frequency from solar polar orbit. J. Adv. Space Res. (2011), doi:10.1016/j.asr.2011.05.001

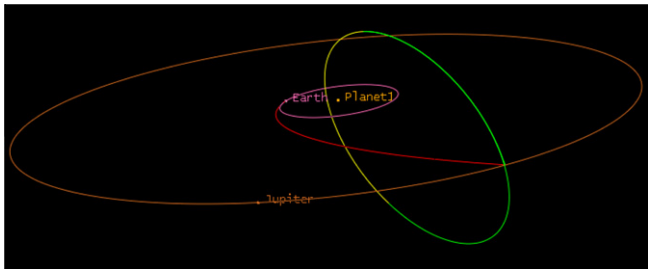

Fig. 10. The solar polar orbit of SPORT.

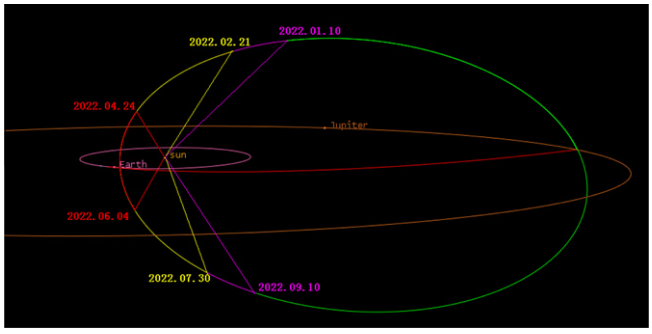

Fig. 11. The general voyage schedule of SPORT.

The launch time for SPORT is proposed in 2019. The preliminary orbit designed shows that the Earth parking orbit altitude is 200 km and the Earth escape velocity increment is about 7.7 km/s. The cruising time from the Earth to Jupiter is about 466 days. After swing-by from Jupiter, the orbit parameters of the solar polar orbit of SPORT are as follows: the orbit inclination of 89.96°, the aphelion altitude of 5.4 AU, and the perihelion altitude of 0.52 AU, the orbit period of 5 years.

The imagining schedule of SPORT is shown in Fig. 11. In the solar polar orbit, the distance between SPORT and the Sun is less than 2AU from January 10 to September 10, 2022. And about on January 10 the interferometric synthetic aperture radiometer will deploy and begin to work. From February 21 to July 30 the distance between SPORT and the Sun is less than 1.5 AU. And the time for the latitude of SPORT less than 60° is from April 24 to June 4. So the best time to get the interferometric imaging from the northern hemisphere is between February 21 and April 24. And the best imaging time from the southern hemisphere is between June 4 and July 30. If the life time of SPORT can last another 5 years, it will get another imaging time similar to above.

8. Scientific objectives and other payloads

SPORT provides an exciting opportunity to explore and characterize the propagation of interplanetary CMEs. The primary objective of the SPORT mission is to observe the propagation of interplanetary CMEs to distances of near 0.35 AU from the Sun. Other important goals of the SPORT mission are the following:

(1) Establish a physical model and prediction model of the chain reaction in response to CMEs and related interplanetary disturbances through solar-terrestrial interplanetary space.
(2) Detect the composition and global spatial distribution of low-energy ions of the solar wind; study the causes and mechanisms of solar wind acceleration, heating and super radial expansion in the solar high-latitude region.
(3) Detect the composition, energy spectrum and flux of high-energy particles of the solar wind at the solar high-latitude region.
(4) Detect the spatial distribution of the interplanetary magnetic field.
(5) Detect short-duration solar radio bursts and carry out joint analyses with other missions such as that located at the L1 point.
(6) Study the interactional process between magnetic field and corona plasmas.
(7) Forecast CMEs for geospace and other interplanetary missions by providing timely images and movies.

The primary scientific payload of the SPORT mission is the interferometric imaging radiometer, which is used to trace the propagation of CMEs through solar-terrestrial interplanetary space. SPORT can also accommodate other payloads to accomplish the other scientific objectives:

(1) A solar X-EUV imaging telescope, which is used to observe solar surface activities from high latitude.
(2) A solar wind ion detector, which is used to detect the composition and global spatial distribution of low-energy ions of the solar wind.
(3) An energetic particle detector, which is used to detect the composition, energy spectrum and flux of high-energy particles of the solar wind.
(4) A fluxgate magnetometer, which is used to detect the spatial distribution of the interplanetary magnetic field.
(5) A low frequency wave detector, which is used to detect interplanetary EM waves.
(6) A solar radio burst spectrometer, which is used to detect short-duration solar radio bursts.

9. Summary

In the years since their discovery, CMEs have come to be recognized as an important means of energy release in the solar corona. Halo CMEs, in particular, are recognized as the major driver of physical conditions in the Sun–Earth system. Consequently, the study of CMEs is important for understanding and ultimately predicting space weather conditions.

Please cite this article in press as: Wu, J., et al. Imaging interplanetary CMEs at radio frequency from solar polar orbit. J. Adv. Space Res. (2011), doi:10.1016/j.asr.2011.05.001

For many years, observations of CMEs have provided the basis for investigating solar-terrestrial interplanetary space. It is worthy to note, that NASA's STEREO mission can obtain stereoscopic imaging of an Earth – impacting solar coronal mass ejection. STEREO mission provides a unique and revolutionary view of the Sun–Earth system. Many problems remain, however, in spite of observations at the L1 point and other in situ data. Observational data on CMEs have not been obtained by space-based instruments beyond the ecliptic plane, and the current statistical models of the propagation of CMEs have not been fully verified. The data on interplanetary CMEs obtained by current instruments cannot fully satisfy the requirements of space weather study and forecast.

The SPORT (Solar Polar Orbit Radio Telescope) mission is proposed to image interplanetary CMEs and to follow their propagation using interferometric imaging technology at the radio wave band from solar polar orbit. The conceptual study and feasibility analyses of SPORT have been financially supported by the Natural Science Foundation of China, the National Space Administration of China and the Chinese Academy of Sciences. Although many problems remain to be solved to implement the SPORT mission, the key topics discussed here are essential for further progress. Engineering design is now underway. If all goes well, the engineering phase of SPORT should begin within two years, as the 2018–2019 launch date is approaching. SPORT will be an important spacecraft dedicated to solar observations and provide a completely new perspective of CMEs.

Acknowledgment

This research work is supported by The Natural Science Foundation of China (Nos. 40574070 and 40671121).

References

Asai, K., Kojima, M., Tokumaru, M., et al. Heliospheric tomography using interplanetary scintillation observations – 3. Correlation between speed and electron density fluctuations in the solar wind. Journal of Geophysical Research 103 (A2), 1991–2001, 1998.

Beatty, P.J., Nishimura, D.G., Pauly, J.M. Rapid gridding reconstruction with a minimal oversampling ratio. IEEE Transactions on Medical Imaging 24 (6), 799–808, 2005.

Bothmer, V., Daglis, I.A. Space Weather – Physics and Effects. Springer, Berlin, 2007.

Brueckner, G.E., Howard, R.A., Koomen, M.J., et al. The large angle spectroscopic coronagraph (LASCO). Solar Physics 162, 357–402, 1995.

Davis, C.J., Davies, J.A., Lockwood, M., et al. Stereoscopic imaging of an Earth – impacting solar coronal mass ejection: a major milestone for the STEREO mission. Geophysical Research Letters 36 (8), L08102.1–L08102.5, 2009.

Doschek, G.A. Solar instruments on the P78-1 spacecraft. Solar Physics 86 (1-2), 9–17, 1983.

Howard, R.A., Moses, J.D., Vourlidas, A., et al. Sun Earth connection coronal and heliospheric investigation (SECCHI). Space Science Reviews 136 (1-4), 67–115, 2008.

Gopalswamy, N.S., Yashiro, G., Michalek, M.L., et al. Interacting coronal mass ejections and solar energetic particles. The Astrophysical Journal 572, L103–L107, 2002.

Gosling, J.T., Hildner, E., MacQueen, R.M., et al. Mass ejection from the Sun – a view from Skylab. JGR 79, 4581–4587, 1974.

Jackson, B.V. Imaging of coronal mass ejections by the Helios spacecraft. Solar Physics 100, 563–574, 1985.

Kahler, S.W., Reames, D.V., Sheeley Jr, N.R. Coronal mass ejections associated with impulsive solar energetic particle events. The Astrophysical Journal 562, 558–565, 2001.

Kivelson, M., Russell, C. Introduction to Space Physics. Cambridge University Press, Cambridge, 1995.

Lario, D. Advances in modeling gradual solar energetic particle events. Advances in Space Research 36, 2279–2288, 2005.

Leblanc, Y., Dulk, G.A., Bougeret, J.-L. Tracing the electron density from the corona to 1 AU. Solar Physics 183, 165–180, 1998.

Lemarchand, G.A. Is there intelligent life out there? Scientific American Quarterly Special Issue on Exploring Intelligence 9 (4), 96–104, 1998.

Lepping, R.P., Burlaga, L.F., Jones, J.A. Magnetic field structure of interplanetary magnetic clouds at 1 AU. Journal Geophysics Research 95, 11957–11965, 1990.

Lugaz, N., Hernandez-Charpak, J.N., Roussev, I.I., et al. Determining the azimuthal properties of coronal mass ejections from multi-spacecraft remote-sensing observations with STEREO SECCHI. The Astrophysical Journal 715, 493–499, 2010.

MacQueen, R.M., Csoeke-Poeckh, A., Hildner, E., et al. The high altitude observatory coronagraph/polarimeter on the solar maximum mission. Solar Physics 65, 91–107, 1980.

Manning, R., Dulk, G.A. The galactic background radiation from 0.2 to 13.8 MHz. Astronomy and Astrophysics 372, 663–666, 2001.

Markus, J.A. Physics of the Solar Corona: An Introduction. Springer-Verlag, Berlin, pp. 703–737, 2004.

Mewaldt, R.A. Solar energetic particle composition, energy spectra, and space weather. Space Science Reviews 124, 303–316, 2006.

Michels, D.J., Howard, R.A., Koomen, M.J., et al. Satellite observations of the outer corona near sunspot maximum. Radio Physics of the Sun 86, 439–442, 1980.

Ramaty, R. Gyrosynchrotron emission and absorption in a magnetoactive plasma. The Astrophysical Journal 158, 753–770, 1969.

RUF, C.S., SWIFT, C.T., TANNER, A.B., et al. Interferometric synthetic aperture microwave radiometry for the remote sensing of the earth. IEEE Transactions on Geoscience and Remote Sensing 26, 597–611, 1988.

Srivastava, N., Venkatakrishnan, P. Relation between CME speed and geomagnetic storm intensity. Geophysical Research Letters 29 (9), 1287–1291, 2002.

Sironi, G., Celora, L. Absolute measurements of the cosmic-background radiation at low frequencies. Il Nuovo Cimento 105 (8–9), 1031–1039, 1990.

Sittler, E.C., Scudder, J.D. An empirical polytrope law for solar wind thermal electrons between 0 45 and 4.76 AU: Voyage 2 and Mariner 10.. Journal of Geophysical Research 85, 5131–5137, 1980.

St Cyr, O.C., Burkepile, J.T. A catalogue of mass ejections observed by the solar maximum mission coronagraph. NCAR Technical Note 352, 1990.

Sun, Weiying, Wu, Ji A study of the bremsstrahlung of plasma at about 1 A U. in times of quiet sun and flare activity. Chinese Astronomy and Astrophysics 29, 149–158, 2005.

Tappin, S.J., Buffington, A., Cooke, M.P., et al. Tracking a major interplanetary disturbance with SMEI. Geophysical Research Letters 31, L02802.1–L02802.4, 2004.

Thompson, A.R., Moran, J.M., Swenson, G.W. Interferometry and Synthesis in Radio Astronomy. John Wiley & Sons, New York, 1986.

Tu, C.Y. Solar-terrestrial Space Physics. Science Press, Beijing, 1988.

Webb, D.F., Mizuno, D.R., Buffington, A., et al. Solar mass ejection imager (SMEI) observations of coronal mass ejections (CMEs) in the heliosphere. Journal of Geophysical Research 111, A12101.1–A12101.19, 2006.

Please cite this article in press as: Wu, J., et al. Imaging interplanetary CMEs at radio frequency from solar polar orbit. J. Adv. Space Res. (2011), doi:10.1016/j.asr.2011.05.001

Wu, C.S., Reiner, M.J., Yoon, P.H., et al. On low-frequency type III solar radio bursts observed in interplanetary space. The Astrophysical Journal 605, 503–510, 2004.

Wu, J., Zhang, C., Liu, H., et al. Clock scan of imaging interferometric radiometer and its applications, in: Proceedings of IGARSS'07, pp. 5244–5246, 2007.

Vourlidas, A. Radio observations of coronal mass ejections. Solar and Space Weather Radiophysics 314, 223–242, 2006.

Yao, Jinxing, Yu, Xingfeng The relation between the energy spectral index of X-ray-producing electrons and that of radio-producing electrons. Acta Astronomica Sinica 39 (4), 398–404, 1998.

Zhang, C., Wu, J., Sun, W.Y. Applications of pseudo-polar FFT in synthetic aperture radiometer imaging, in: Progress in Electromagnetic Research Symposium (PIERS) Online, vol. 3, pp. 25–30, 2007.

Please cite this article in press as: Wu, J., et al. Imaging interplanetary CMEs at radio frequency from solar polar orbit. J. Adv. Space Res. (2011), doi:10.1016/j.asr.2011.05.001